arXiv:1606.09477v2 [cond-mat.supr-con] 2 Jul 2016

Comparative study of high-T_c superconductivity in H_3S and H_3P

Hyungju Oh,* Sinisa Coh, and Marvin L. Cohen
Department of Physics, University of California at Berkeley and Materials Sciences Division, Lawrence Berkeley National Laboratory, Berkeley, California 94720, USA
(Dated: July 5, 2016)

We report on a comparative study of the electronic structure, phonon spectra, and superconducting properties for recently discovered superconducting hydrides, H_3S and H_3P. While the electronic structures of these two materials are similar, there are notable changes in the phonon spectra and electron-phonon coupling. The low-frequency bond-bending modes are softened in H_3P and their coupling to the electrons at the Fermi surface is enhanced relative to H_3S. Nevertheless, coupling to the high-frequency modes is reduced so the resulting calculated superconducting transition temperature is reduced from ∼166 K in H_3S to ∼76 K in H_3P.

PACS numbers: 71.15.Mb, 71.20.-b, 74.20.Fg, 74.62.Bf

I. INTRODUCTION

Many materials have been proposed theoretically as conventional phonon-mediated superconductors having a high superconducting transition temperature (T_c). Based on the BCS theory[1], materials with light masses and strong bonds are promising candidates for high-T_c superconductors[2,3] because T_c is scaled by the inverse square root of the atomic mass. Therefore, theoretical studies have been intensively performed focusing on the compounds consisting of the lightest hydrogen atom. In experiments, on the other hand, achieving a high-T_c in hydrogen compounds has not been reported yet. Recently, it is experimentally reported that, under extreme high pressures of 100–200 GPa, sulfur hydride transforms to a metallic state and shows extremely high-T_c up to ∼200K[4,5].

To find out the crystal structure of the high-T_c sulfur hydride, many *ab-initio* studies have been done and most of these studies have concluded that cubic H_3S will form with a H-rich decomposition environment under high pressure[6–12]. Furthermore, from electron-phonon coupling (EPC) calculations[6–15], it is revealed that strong coupling happens between high-frequency phonon modes and electrons and these strong coupling induces high-T_c in the body-centered cubic H_3S.

Here we study two types of hydrides, H_3S and H_3P. Following the discovery of high-T_c conventional superconductivity in sulfur hydride, a hydride phosphine (H_3P) was also reported to be a possible high-T_c ($T_c > 100$ K at pressure P> 200 GPa) superconductor via four-probe electrical measurements[16]. Hence we compare the normal and superconducting properties of these two materials. For the crystal structures of high-T_c hydrides, X-ray diffraction experiments[12,17] confirm that the sulfur atoms of H_3S form a body-centered cubic structure as shown in Fig. 1. Up to now, no available experimental data for the crystal structure of H_3P exists. Hence for comparison purposes, we assume in this study that both materials have the same crystal structure and analyze the effect of element change on material properties.

II. METHODS

The following methods are used to perform the calculations of the electronic structures, phonon properties, and superconducting properties. For the electronic structures, our calculations are based on *ab-initio* norm-conserving pseudopotentials and the Perdew-Burke-Ernzerhof[18] functional as implemented in the SIESTA[19] and Quantum-ESPRESSO[20] codes. Phonon frequencies are computed using density-functional perturbation theory[21] implemented in Quantum-ESPRESSO[20] package. Finally, EPC and Eliashberg spectral functions are obtained via the Wannier90[22] and EPW[23] packages.

For the calculation using SIESTA, electronic wavefunctions are expanded with pseudoatomic orbitals (double-ζ polarization) and a charge density cutoff of 800 Ry is used. We sample the Brillouin zone on a uniform 16×16×16 k-point mesh. For the calculation with Quantum-ESPRESSO, a plane-wave basis up to 160 Ry and a 32×32×32 k mesh size are employed.

Phonon frequencies $\omega_{\mathbf{q}\nu}$ and EPC parameters $\lambda_{\mathbf{q}\nu}$ are computed on a coarse mesh (8×8×8) of reciprocal space. Next, interpolation techniques[24] based on maximally localized Wannier functions[24–26] are used to interpolate EPC parameters on a fine grid (36×36×36).

The Eliashberg spectral function $\alpha^2F(\omega)$ is computed by integrating the interpolated phonon frequencies $\omega_{\mathbf{q}\nu}$ and the EPC $\lambda_{\mathbf{q}\nu}$ over the Brillouin zone,

$$\alpha^2F(\omega) = \frac{1}{2}\sum_{\mathbf{q}\nu} \mathrm{w}_{\mathbf{q}}\omega_{\mathbf{q}\nu}\lambda_{\mathbf{q}\nu}\delta(\omega-\omega_{\mathbf{q}\nu}). \qquad (1)$$

Here the $\mathrm{w}_{\mathbf{q}}$ is the Brillouin zone weight associated with the phonon wavevectors $\mathbf{q}$. The total EPC λ is calculated as the Brillouin zone average of the mode-resolved coupling strengths $\lambda_{\mathbf{q}\nu}$:

$$\lambda = \sum_{\mathbf{q}\nu} \mathrm{w}_{\mathbf{q}}\lambda_{\mathbf{q}\nu} = 2\int_0^\infty d\omega\ \alpha^2F(\omega)/\omega. \qquad (2)$$

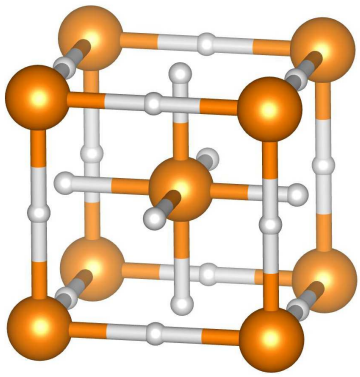

FIG. 1. The $Im\bar{3}m$ crystal structure assumed for H_3S and H_3P. The large sphere (orange) is S or P, and the small sphere (white) is H.

III. ELECTRONIC STRUCTURE

Here we discuss the electronic structure of H_3S and H_3P. In all of our calculations we set the conventional lattice parameter as 3 Å. With this lattice parameter, the calculated pressures of both materials are 220 GPa.

The overall shapes of the band structures are similar for both materials [Figs. 2(a) and (c)]. Because phosphorus has one less valence electron than sulfur, the Fermi level (E_F) is shifted down in H_3P. With the shift, E_F of H_3P is placed near a different peak position in the density of states (DOS). For H_3S, the DOS at E_F is calculated to be 0.45 states eV^{-1} $f.u.^{-1}$. A similar value (0.50 states eV^{-1} $f.u.^{-1}$) for the DOS is found in the case of H_3P.

Figure 2 compares the orbital contributions to the band structure and DOS in H_3S and H_3P. In both materials, the DOS at E_F comes dominantly from $3p$ orbitals of sulfur or phosphorus. The portion of $3p$ orbitals is twice as large as the portion of hydrogen orbitals. The Fermi surfaces originated from hydrogen orbitals are almost same in both case, forming small hole pockets centered at Γ-point.

IV. PHONON PROPERTIES

In this section we discuss the differences of the phonon properties between H_3S and H_3P. When the sulfur is changed to phosphorus, the characteristics of the phonon spectra differ significantly along Γ–H and H–N high-symmetry lines [Fig. 3]. The hydrogen–phosphorus bond-bending modes become softer and three unstable phonon modes appear at the H high-symmetry point. Therefore we expect that in the doubled unit cell these unstable modes would be stabilized. We exclude these negative phonon modes when calculating α^2F so that we can make an reliable comparison with H_3S. The structural instability of body-centered cubic H_3P is also reported

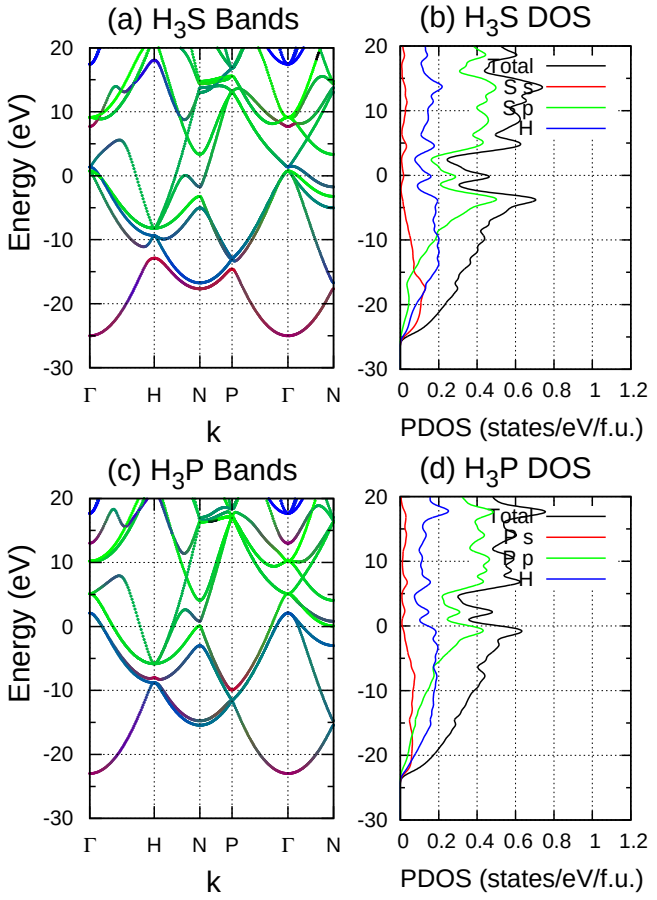

FIG. 2. Electronic band structures and density of states (DOS) per three-hydrogen formula unit (f.u.) of (a), (b) H_3S and (c), (d) H_3P. Dominant orbital characters are represented in blue (H orbitals), red (S or P s orbitals), and green (S or P p orbitals) color.

by previous theoretical structural studies[27,28].

Next we discuss the strength of the EPC for the two cases. In H_3S, phonon modes of 150∼200 meV frequencies (which are H–S bond-stretching modes) are strongly coupled to electrons at the Fermi surface. In H_3P, however, low-frequency modes (< 50 meV) are more relevant. These modes originate from softened H–P bond-bending motion.

To give a more quantitative discussion about the relevant energy scales of the phonons, we calculate the EPC-weighted average of the phonon frequencies,

$$\omega_{\ln} = \exp\left\{\frac{2}{\lambda}\int_0^\infty d\omega\ \frac{\alpha^2F(\omega)}{\omega}\ \ln\omega\right\}. \qquad (3)$$

The value of $\omega_{\ln}$ is 1580 K (136 meV) for the H_3S and 610 K (53 meV) for the H_3P. Therefore $\omega_{\ln}$ is more than twice as large in H_3S relative to H_3P.

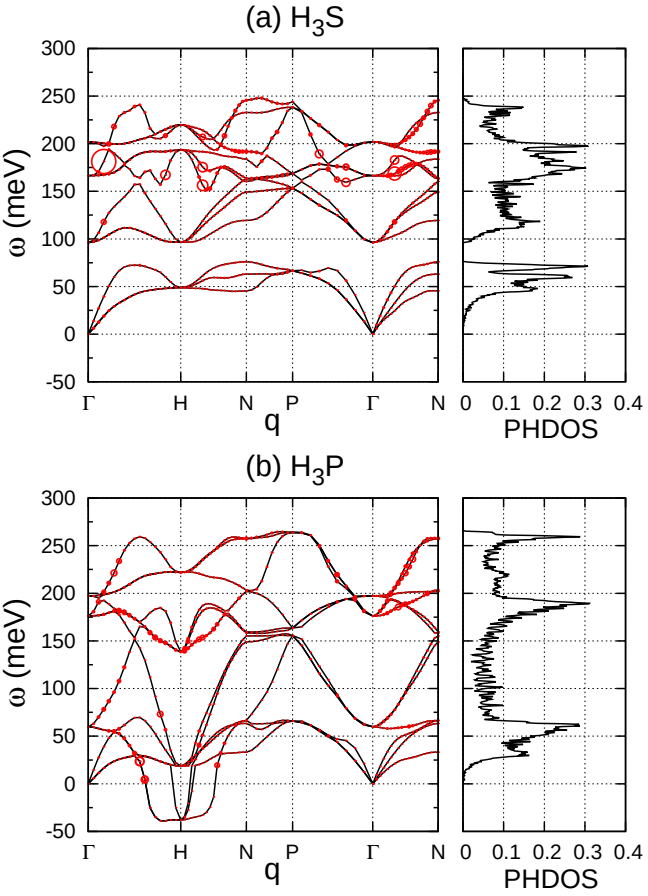

FIG. 3. Phonon spectrum and phonon density of states (PHDOS) of (a) H_3S and (b) H_3P. The radius of the red circle is proportional to $\omega_{\mathbf{q}\nu}\lambda_{\mathbf{q}\nu}$.

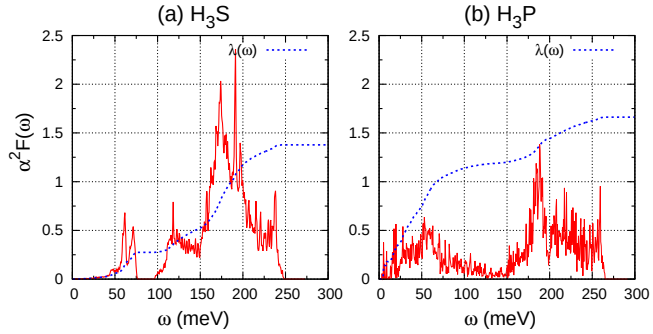

FIG. 4. Eliashberg spectral function α^2F (red) and cumulative contribution to the electron-phonon coupling strength λ (blue) of (a) H_3S and (b) H_3P. The cumulative EPC is calculated as $\lambda(\omega) = 2\int_0^\omega d\omega'\ \alpha^2F(\omega')/\omega'$.

V. SUPERCONDUCTING PROPERTIES

The total EPC λ equals 1.38 in H_3S, whereas it reaches 1.66 in H_3P. The Eliashberg phonon spectral functions of H_3S and H_3P are quite different. The EPC in H_3S is dominated by the phonon modes at the zone center Γ point. In H_3P, however, we observed an overall contribution of different modes to λ along Γ–H–N directions as shown in Fig. 3.

Here we discuss why there is a large difference in the EPC between H_3S and H_3P. First, we consider the difference in DOS. Since λ is roughly proportional to the DOS at E_F, the EPC could be enhanced by the large DOS. However, in our case, there is no sufficient change in DOS to reproduce the large enhancement in EPC for H_3P. Another point is the coupling strength between the electrons and the low-frequency hydrogen vibration. There is no significant enhancement in the electron-phonon matrix elements which is proportional to $\omega_{\mathbf{q}\nu}\lambda_{\mathbf{q}\nu}$ [Fig. 3]. But, the dominant modes to EPC appear at low frequencies in H_3P [Fig. 4]. This change causes the enhancement of the EPC λ value.

Finally, we estimate the superconducting transition temperature T_c using the McMillan equation[29]

$$T_c = \frac{\omega_{\ln}}{1.20}\exp\left\{-\frac{1.04\ (1+\lambda)}{\lambda-\mu^*(1+0.62\ \lambda)}\right\}. \qquad (4)$$

Here μ^* is the Coulomb repulsion parameter. For commonly used $\mu^* = 0.1$ we estimate $T_c = 166$ K for H_3S and 76 K for H_3P. The exact value of μ^* here is not that important since even with $\mu^* = 0$ we get very similar T_c (219 and 96 K).

The value of λ we obtained for H_3S and H_3P is near the limit of applicability of the McMillan equation. However, we find that the Kresin–Barbee–Cohen model[30,31], which is applicable for large λ, gives similar estimates for T_c.

Although H_3P has a higher λ value than H_3S, the estimated T_c is about half of that in H_3S. This agrees well with the experimentally obtained T_c of $\sim$ 200 K in H_3S and $\sim$ 100 K in H_3P. We expect that the deviation here from experiment might occur because we ignored unstable phonon modes in our calculation, so softening might be overestimated for H_3P in the low-frequency regime.

VI. CONCLUSION

With the assumption of the same body-centered cubic structure and lattice parameter, we compare the electronic, phonon, and superconducting properties of H_3S and H_3P. The results of electronic structures show no significant difference, except for a slight change in the Fermi level due to the different number of valence electrons. However, there are notable changes in phonon spectrum and electron-phonon coupling properties. First, there exists phonon softening in low-frequency bond-bending modes, and the coupling of these modes to electrons near the Fermi surface is enhanced. As the dominant frequency regime changes from high to low frequency, the superconducting transition temperature is reduced from $\sim$166 K in H_3S to $\sim$76 K in H_3P.

ACKNOWLEDGEMENTS

This work was supported by National Science Foundation Grant No. DMR15-1508412 (electronic structure calculation) and by the Director, Office of Science, Office of Basic Energy Sciences, Materials Sciences and Engineering Division, U.S. Department of Energy under Contract No. DE-AC02-05CH11231, within the Theory Program (phonon and superconducting properties calculations). Computational resources have been provided by the DOE at Lawrence Berkeley National Laboratory's NERSC facility.

* Email: xtom97@gmail.com

[1] J. Bardeen, L. N. Cooper, and J. R. Schrieffer, Phys. Rev. **108**, 1175 (1957).
[2] J. E. Moussa and M. L. Cohen, Phys. Rev. B **78**, 064502 (2008).
[3] M. L. Cohen, Modern Phys. Lett. B **24**, 2755 (2010).
[4] A. P. Drozdov, M. I. Eremets, I. A. Troyan, V. Ksenofontov, and S. I. Shylin, Nature (London) **525**, 73 (2015).
[5] I. Troyan, A. Gavriliuk, R. Rüffer, A. Chumakov, A. Mironovich, I. Lyubutin, D. Perekalin, A. P. Drozdov, and M. I. Eremets, Science **351**, 1303 (2016).
[6] D. Duan, Y. Liu, F. Tian, D. Li, X. Huang, Z. Zhao, H. Yu, B. Liu, W. Tian, and T. Cui, Sci. Rep. **4**, 6968 (2014).
[7] H. Wang, J. S. Tse, K. Tanaka, T. Iitaka, and Y. Ma, Proc. Natl. Acad. Sci. U.S.A. **109**, 6463 (2012).
[8] I. Errea, M. Calandra, C. J. Pickard, J. Nelson, R. J. Needs, Y. Li, H. Liu, Y. Zhang, Y. Ma, and F. Mauri, Phys. Rev. Lett. **114**, 157004 (2015).
[9] N. Bernstein, C. S. Hellberg, M. D. Johannes, I. I.Mazin, and M. J. Mehl, Phys. Rev. B **91**, 060511(R) (2015).
[10] D. Duan, X. Huang, F. Tian, D. Li, H. Yu, Y. Liu, Y. Ma, B. Liu, and T. Cui, Phys. Rev. B **91**, 180502(R) (2015).
[11] Y. Li, L. Wang, H. Liu, Y. Zhang, J. Hao, C. J. Pickard, J. R. Nelson, R. J. Needs, W. Li, Y. Huang, I. Errea, M. Calandra, F. Mauri, and Y. Ma, Phys. Rev. B **93**, 020103(R) (2016).
[12] I. Errea, M. Calandra, C. J. Pickard, J. R. Nelson, R. J. Needs, Y. Li, H. Liu, Y. Zhang, Y. Ma, and F. Mauri, Nature (London) **532**, 81 (2016).
[13] D. A. Papaconstantopoulos, B. M. Klein, M. J. Mehl, and W. E. Pickett, Phys. Rev. B **91**, 184511 (2015).
[14] C. Heil and L. Boeri, Phys. Rev. B **92**, 060508(R) (2015).
[15] W. Sano, T. Koretsune, T. Tadano, R. Akashi, and R. Arita, Phys. Rev. B **93**, 094525 (2016).
[16] A. P. Drozdov, M. I. Eremets, and I. A. Troyan, arXiv:1508.06224.
[17] M. Einaga, M. Sakata, T. Ishikawa, K. Shimizu, M. I. Eremets, A. P. Drozdov, I. A. Troyan, N. Hirao, and Y. Ohishi, arXiv:1509.03156.
[18] J. P. Perdew, K. Burke, and M. Ernzerhof, Phys. Rev. Lett. **77**, 3865 (1996).
[19] D. Sánchez-Portal, P. Ordejón, E. Artacho, and J. M. Soler, Int. J. Quantum Chem. **65**, 453 (1997).
[20] P. Giannozzi *et al.*, J. Phys.: Condens. Matter **21**, 395502 (2009).
[21] S. Baroni, S. de Gironcoli, A. Dal Corso, and P. Giannozzi, Rev. Mod. Phys. **73**, 515 (2001).
[22] A. A. Mostofi, J. R. Yates, Y.-S. Lee, I. Souza, D. Vanderbilt, and N. Marzari, Comput. Phys. Commun. **178**, 685 (2008).
[23] J. Noffsinger, F. Giustino, B. D. Malone, C.-H. Park, S. G. Louie, and M. L. Cohen, Comput. Phys. Commun. **181**, 2140 (2010).
[24] F. Giustino, M. L. Cohen, and S. G. Louie, Phys. Rev. B **76**, 165108 (2007).
[25] N. Marzari and D. Vanderbilt, Phys. Rev. B **56**, 12847 (1997).
[26] I. Souza, N. Marzari, and D. Vanderbilt, Phys. Rev. B **65**, 035109 (2001).
[27] A. Shamp, T. Terpstra, T. Bi, Z. Falls, P. Avery, and E. Zurek, J. Am. Chem. Soc. **138**, 1884 (2016).
[28] H. Liu, Y. Li, G. Gao, J. S. Tse, and I. I. Naumov, J. Phys. Chem. C **120**, 3458 (2016).
[29] P. Allen and R. Dynes, Phys. Rev. B **12**, 905 (1975).
[30] V. Z. Kresin, Bull. Am. Phys. Soc. **32**, 796 (1987).
[31] L. C. Bourne, A. Zettl, T. W. Barbee III, and M. L. Cohen, Phys. Rev. B **36**, 3990 (1987).